Accepted: 28 March 2022

DOI: 10.1002/lsm.23548

BASIC SCIENCE

Nondestructive optical feedback systems for use during infrared laser sealing of blood vessels

Nicholas C. Giglio PhD | **Nathaniel M. Fried PhD**

Department of Physics and Optical Science, University of North Carolina at Charlotte, Charlotte, North Carolina, USA

Correspondence

Nathaniel M. Fried, PhD, Department of Physics and Optical Science, University of North Carolina at Charlotte, 9201 University City Blvd, Charlotte, NC 28223, USA.
Email: nmfried@uncc.edu

Funding information

National Institute of Biomedical Imaging and Bioengineering, Grant/Award Number: R15EB028576

Abstract

Objectives: High-power infrared lasers are capable of sealing blood vessels during surgery. A real-time diagnostic feedback system utilizing diffuse optical transmission is characterized by nondestructive identification of vessel seals.

Materials and Methods: For real-time diffuse optical transmission experiments, two approaches were studied. First, a low-power (1.2 mW) visible aiming beam (635 nm) was used for diagnostics, co-aligned with the therapeutic high-power infrared beam (1470 nm). Second, the 1470 nm beam was used simultaneously for both therapy and diagnostics. For both studies, the 1470-nm laser delivered 5 W for 5 seconds for unsuccessful seals (control) versus 30 W for 5 seconds for successful seals, using a linear beam profile (8.4 × 2 mm). Diffuse optical transmission signals were correlated with vessel burst pressures measured using a standard burst pressure setup.

Results: Diffuse optical transmission studies using the low-power, 635-nm aiming beam were promising. A decrease in the visible transmitted signal of 59 ± 11% was measured for successful seals versus 23 ± 8% for failed seals ($p = 5.4E{-}8$). The use of the high-power, 1470-nm infrared laser for simultaneous therapeutics and diagnostics proved inconsistent and unreliable, due in part to the dynamic and rapid changes in water content and absorption during the seal.

Conclusions: A low-power, visible aiming beam, integrated with the therapeutic high-power infrared diode laser, may be used as a real-time diagnostic system for indicating successful laser seals, based on significant changes in optical scattering and diffuse optical transmission between native and coagulated compressed vessels. With further development, this simple and inexpensive optical feedback system may be integrated into a laparoscopic device for laser de-activation upon successful vessel sealing.

KEYWORDS

artery, blood vessel, coagulation, feedback, fusion, infrared, laser, seal, transmission

INTRODUCTION

Electrosurgical radiofrequency (RF) and ultrasonic (US) devices are used to replace suture ligation for expediting sealing with hemostasis and bisection of vascular tissues in about 80% of the approximately 15 million laparoscopic surgical procedures performed globally each year.[1] It is common for these conventional energy-based devices to incorporate real-time diagnostic feedback during surgery, primarily in the form of electrical impedance measurements and/or temperature sensors.[2–4] This real-time feedback enables the surgeon to confirm that a strong vessel

Part of this study was published as a conference proceedings paper at the 2021 SPIE European Conferences on Biomedical Optics and as a conference proceedings paper at the 2022 SPIE Photonics West International Symposium on Biomedical Optics.

This is an open access article under the terms of the Creative Commons Attribution-NonCommercial-NoDerivs License, which permits use and distribution in any medium, provided the original work is properly cited, the use is non-commercial and no modifications or adaptations are made.
© 2022 The Authors. *Lasers in Surgery and Medicine* published by Wiley Periodicals LLC.

seal has been achieved and may also serve as a closed feedback loop for automating energy delivery, thus saving valuable operating room time.

An optical method has recently been tested experimentally as an alternative to RF and US devices, both ex vivo and in vivo, during preclinical studies, using a high-power, 1470-nm, infrared (IR) diode laser for thermal sealing and bisection of blood vessels.[5–8] This promising optical technique has produced stronger seals in shorter times and with less thermal spread than reported using RF and US devices.[6]

Several previous experimental studies have reported the use of optical-based methods as potential diagnostic approaches to differentiate between native and coagulated tissue for RF tissue fusion.[9–12] However, the majority of these studies relied on relatively complex spectroscopic methods for feedback.

Our laboratory has recently demonstrated a simple and inexpensive alternative technique, using a diffuse optical transmission method for measuring a reduced signal after IR laser sealing of vessels.[13] Successful seals (as defined by vessel burst pressures [BPs] ≥ 360 mmHg) experienced a decrease in diffuse transmitted IR laser power of 56 ± 25% versus a decrease in power of only 31 ± 24% for failed seals ($p = 7.2\text{E}{-4}$). However, these studies were not conducted in real-time, with measurements only made before and after IR laser sealing was performed.

The objective of this preliminary study is to demonstrate a real-time, nondestructive, diffuse optical transmission method for diagnostic feedback during blood vessel sealing and to correlate the optical signal with a destructive evaluation of blood vessel seals using a standard BP setup. The visible aiming beam (635 nm) integrated into the therapeutic high-power IR diode laser, or alternatively the IR laser beam (1470 nm) itself, is compared for potential use as diagnostic beams.

The feedback system exploits differences in optical transmission signals between native and thermally coagulated vessels. When soft tissues are coagulated, the light scattering coefficient (μ_s) increases significantly, resulting in reduced optical transmission through the tissue.[14–18] Other optical parameters, including light absorption coefficient (μ_a), anisotropy factor or light scattering direction (g), and refractive index (n), experience little or no change.

THEORY

Photon distribution simulations for native and coagulated blood vessels

A Monte Carlo (MC) model using MATLAB code[19–21] was used to observe photon distribution in a blood vessel compressed to a fixed thickness of 400 μm (similar to previous experimental studies[5–8]), before and after IR laser thermal tissue coagulation and to determine if this difference can be used for detection. The MC model is considered a random walk simulation in three-dimensional space. As a photon travels through the model, it moves from one absorption or scattering event to the next, until the photon either exits the tissue sample or becomes fully absorbed by the tissue. The fluence rate pattern exiting the compressed vessel at $r = 400$ μm is calculated by:

$$\delta(r) = \frac{N_a(r)}{\Delta V(r) N \mu_a(r) \zeta},$$

where r is the depth in the sample, $\delta(r)$ is the fluence rate, $N_a(r)$ is the total fractional absorbed packet in a given matrix element and is based on the absorption and scattering and coefficients, $\Delta V(r)$ is the volume of tissue element, N is the total number of photons that enter the simulation, $\mu_a(r)$ is the absorption coefficient, and ζ is the initial weight of each photon.[22]

A homogeneous plane-parallel geometry was used to simulate the distribution of photons deposited in a compressed (flattened) artery. Three million photons were simulated to achieve sufficient (4 μm axial) spatial resolution and distribution of light absorbed in the tissue. Both 1470-nm (near-IR) and 635-nm (visible) wavelengths were simulated since these wavelengths were used in this study for diagnostic purposes.

Figure 1 shows a center slice for both native and coagulated tissue of the MC plots in the vessel for the laser spatial beam profile of 8.4 × 2.0 mm at 1470 and 635 nm. The normalized fluence rate exhibits a peak just below the vessel surface, due to contributions from back-scattered photons, and then follows an exponentially decaying trend, as expected. The decay in fluence rate for the coagulated blood vessel is steeper due to enhanced light scattering effects in coagulated tissue. The discrete optical properties of normal and coagulated aorta under compression were extrapolated from existing literature for all wavelengths used in this study (Figure 1).[17,18]

The figure also provides a calculated percent change of normalized fluence rate at 400 μm between native and coagulated blood vessels for 1470 and 635 nm. This value is the minimum expected decrease in optical transmission signal during experimental studies for IR laser sealing of vessels.

It should be emphasized that the optical properties of blood were intentionally not considered in the MC model for laser tissue fusion described above. During clinical laser vessel sealing, the jaws of the laparoscopic device compress the blood vessel, thus displacing any blood that would normally be flowing through the vessel. Both this vessel compression and laser energy deposition in the tissue are necessary to produce a strong vessel seal.

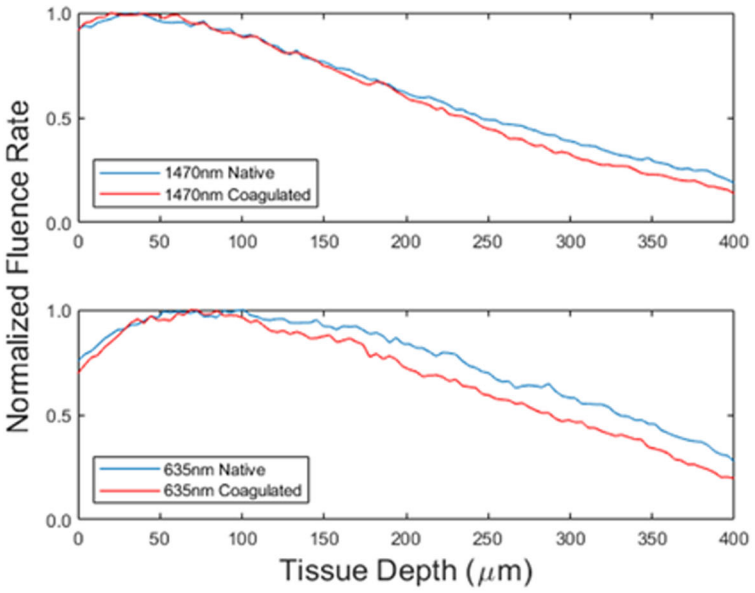

Wavelength, λ (nm)		1470	635
Absorption Coefficient μ_a (cm^{-1})	Native / Coagulated	20.4	1.5
Scattering Coefficient μ_s (cm^{-1})	Native	267	440
	Coagulated	357	590
Anisotropy Factor g	Native / Coagulated	0.875	0.875
Tissue thickness (mm)	Native / Coagulated	0.4	0.4
Simulated Change in Fluence (%)		26	29

FIGURE 1 A center slice of MC simulation after absorption of three million photons in the vessel (compressed to a fixed thickness of 400 μm) using a laser spatial beam profile of 8.4 × 2.0 mm. (Top) Normalized fluence rate 1D plot of 1470 nm for both native and coagulated tissue. (Bottom) Normalized fluence rate 1D plot of 635 nm for both native and coagulated tissue. (Right) Optical properties of native and coagulated compressed blood vessels at 1470 and 635 nm. Calculated percent change in fluence rate at 400 μm penetration depth from native to coagulated state. 1D, one dimensional; MC, Monte Carlo.[17,18]

FIGURE 2 (A) Dissected porcine kidney. (B) Vessel tree showing the medium size (2–4 mm) blood vessels used in this study.

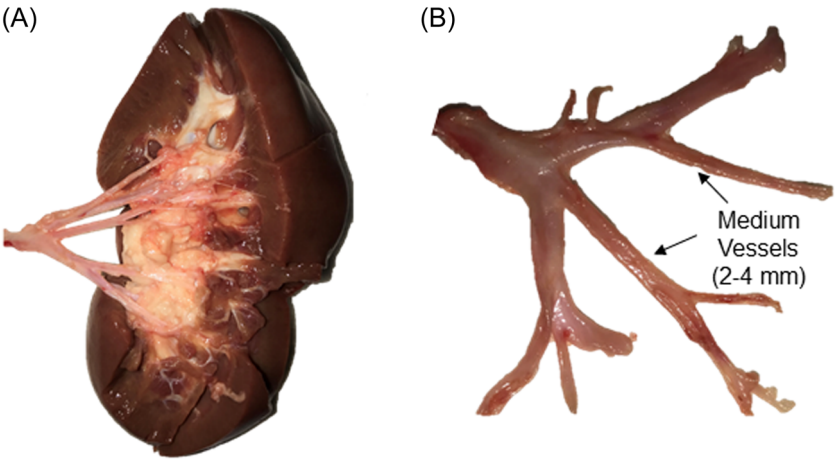

MATERIALS AND METHODS

Tissue preparation

Arteries (2–4 mm in diameter) were surgically dissected from fresh porcine kidney pairs obtained from an abattoir (Spear Products, Inc.) (Figure 2). All blood vessels were stored in saline in a refrigerator (4°C) for no longer than 48 hours before use. Samples were brought to room temperature (20°C) before each experiment was performed.

Optical diffuse transmission experimental setup

Visible laser ($\lambda = 635$ nm)

Experiments utilized a benchtop setup that mirrored a classic Maryland style jaw, potentially utilizing the bottom jaw for therapeutic applications while simultaneously utilizing the top jaw for optical transmission diagnostics. The setup consisted of a 1470-nm laser (BrightLase Ultra-100; QPC Lasers) (for therapeutics) and an integrated co-aligned aiming beam 635 nm (for diagnostics),

delivered via a multimode (MM), 550-μm-core, fiber optic patchcord (FG550LEC-CUSTOM; Thorlabs) with a numerical aperture (NA) of 0.22 and high-power proximal SMA905 connectors, and controlled by a time-gated shutter (Figure 3). The light was then collimated by a 35-mm focal length plano-convex lens to an 8.4 mm diameter beam spot and focused by a cylindrical lens with a 100-mm focal length onto a compressed blood vessel sample. The sample was compressed between a 1-mm glass slide and a custom backplate, which was precision machined to seat a 3-mm glass slide with a 400-μm gap stop for uniform compression. The backplate contained a 1-mm hole open to the glass slide to allow diffuse light from the tissue to be transmitted. The backplate was also machined and threaded to accommodate a subminiature assembly (SMA) fiber connector attachment, which was concentric with the 1-mm through hole for MM fiber connection.

A 1000-μm-core-diameter optical fiber with 0.50 NA was attached to the backplate, which was opposite the vessel from the incident laser beam and collected diffuse transmitted light. A large core, large NA fiber was used to capture the dynamic change in photon scattering during laser irradiation. The fiber output was attenuated and filtered with a short-pass filter, and then focused onto a silicon photodetector (DET110; Thorlabs). Data were then collected via an oscilloscope (Figure 3).

The 1470-nm laser was operated at either 30 W for 5 seconds for successful seals or 5 W for 5 seconds for failed seals (control). The red aiming beam (1.2 mW at 635 nm), co-aligned with the IR beam, was used for real-time optical feedback during sealing. All studies used a linear beam measuring 8.4 × 2.0 mm. Optical signals for successful ($n = 12$) and failed ($n = 12$) seals were correlated with vessel BPs using destructive testing via a standard BP setup.

IR laser ($\lambda = 1470$ nm)

Simultaneous use of the high-power 1470-nm IR laser beam for both therapeutics and diagnostics utilized a similar experimental setup as described above for the visible beam, but with a few modifications. The silicon detector (sensitive to shorter laser wavelengths) was replaced with an indium gallium arsenide (InGaAs) photodetector (PDA400; Thorlabs) for collecting the longer wavelength IR light. The short-pass filter for the visible beam transmission was also replaced with a neutral density filter to attenuate the high-power IR laser beam before its incidence on the photodetector, to prevent optical damage to the photodetector (Figure 3).

BP measurements

After completion of IR laser vessel sealing and non-destructive testing of all vessel seals, standard BP measurements were conducted to determine seal strength (Figure 4). The BP setup consisted of a pressure meter (Model 717 100 G; Fluke), syringe pump (Cole Parmer), and an iris as a clamp. Deionized water was pumped at a rate of 100 ml/hour and maximum pressure was achieved before a seal burst was recorded.

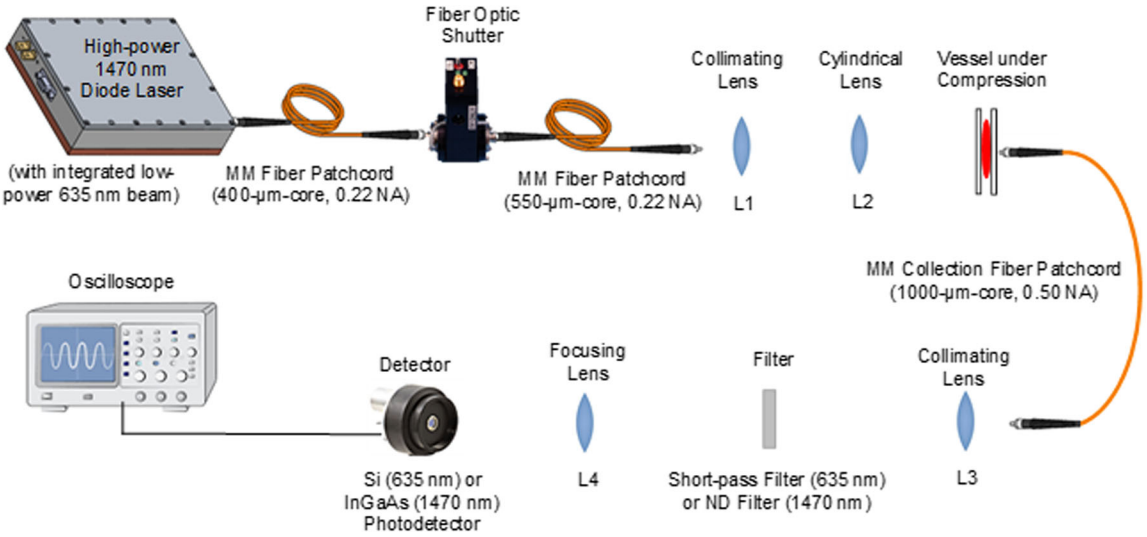

FIGURE 3 Real-time optical transmission setup, with 1470 nm therapeutic/diagnostic, or 635 nm diagnostic beams coupled into a MM fiber with beam shaping via a collimating lens (L1) and cylindrical lens (L2) to form a linear beam profile of 8.4 × 2 mm. The blood vessel sample was clamped with a custom mount, allowing diffusely scattered light to be collected by a MM fiber. The diagnostic beam was collimated (L3), filtered (short-pass filter for 635 nm wavelength or neutral density filter for 1470 nm wavelength), and focused (L4) into a detector (silicon photodetector for 635 nm wavelength or indium gallium arsenide photodetector for 1470 nm wavelength), connected to an oscilloscope. MM, multimode.

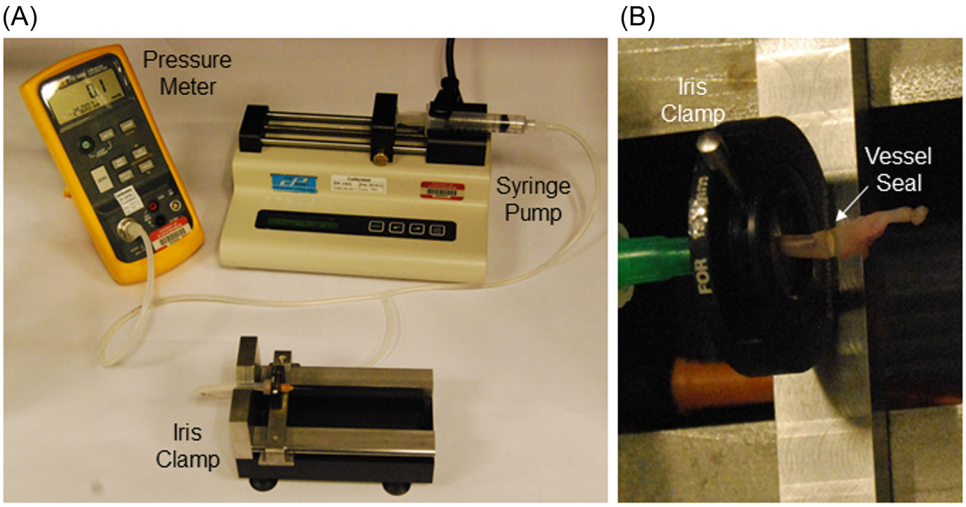

FIGURE 4 (A) The standard vessel burst pressure setup consisted of a pressure meter, syringe pump, and an iris used as a clamp. (B) Magnified image of the iris clamp showing an attached sealed blood vessel in the process of being tested. Deionized water was pumped at a rate of 100 ml/hour and the maximum pressure achieved was recorded. A seal was considered successful if it reached at least three times systolic blood pressure (360 mmHg).

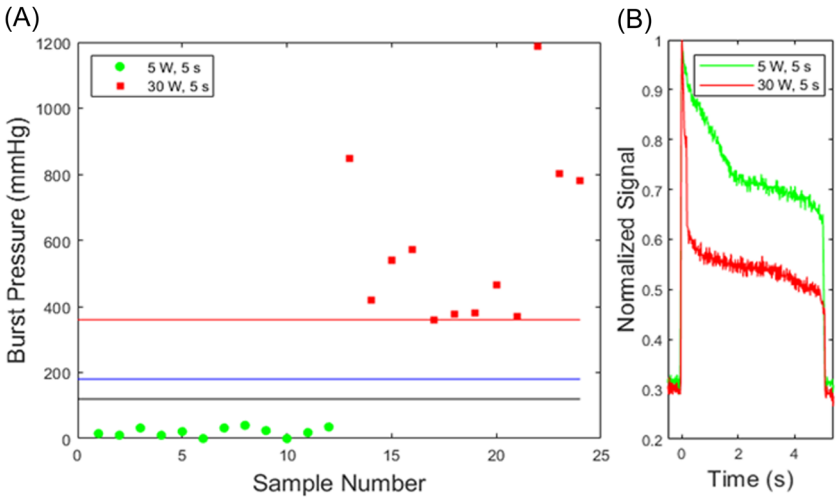

FIGURE 5 (A) Scatter plot showing BP data for 24 vessels tested. Colored data points separate data as a function of laser irradiation time (30 W for 5 seconds and 5 W for 5 seconds), while horizontal colored lines represent criteria for success (360 mmHg), hypertensive blood pressure (180 mmHg), and systolic blood pressure (120 mmHg). (B) Representation of real-time power data acquired during sealing. The green line represents 5 W, 5 seconds seal of a 3.1 mm diameter blood vessel with BP = 10 mmHg (failed seal) and a decrease in the signal of 34%. The red line represents 30 W, 5 seconds seal of a 3.1 mm blood vessel with BP = 540 mmHg (successful seal) and a decrease in the signal of 50%. BP, burst pressure.

Statistical analysis

A threshold BP of 360 mmHg or three times normal systolic blood pressure (120 mmHg) was used, which was consistent with industry standards in the field. Laser-sealed blood vessels with BPs ≥ 360 mmHg were labeled as successful, while BPs < 360 mmHg were considered failures. A two-tailed t test was used in comparing BPs between data sets, with values of $p < 0.01$ considered to be highly statistically significant.

RESULTS

Optical diffuse transmission using visible laser ($\lambda = 635$ nm)

Light scattering increased significantly as vessels were thermally coagulated, leading to a decay in real-time power readings. Figure 5A shows a scatter plot of the BP data for all vessels tested ($n = 24$), with criteria for success (≥360 mmHg), hypertensive blood pressure (180 mmHg),

and systolic blood pressure (120 mmHg) lines marked for reference. Successful seals correlated with a percent decrease in optical transmission signal of 59 ± 11%, while failed seals corresponded to a decrease of only 23 ± 8% ($p = 5.4E{-}8$). The decrease in transmission for failed seals was primarily due to increased scattering of the light from the surface of the partially thermally coagulated vessel. For the vessel lumen to be completely sealed, the scattering coefficient must rise sufficiently to produce an approximately 59% decrease in transmission.

Figure 5B shows a representation of the real-time power data acquired during a sealing procedure. The signal begins with a high amplitude at $t = 0$ seconds, when the laser is first activated, and then continues to decrease, until the laser is de-activated at $t = 5$ seconds. The first, lower power treatment group (5 W for 5 seconds) exhibits a slower rate of decay than that of the second, higher power treatment group (30 W for 5 seconds). The large initial decay in signal observed in Figure 5B in the 30 W group is representative of the initial rapid change in the tissue optical properties and was constant for all samples collected at these settings. Decay in both signals is interpreted to represent a rise in the scattering coefficient during the procedure. As the scattering coefficient increases, photons experiencing more scattering events in the tissue contribute to a larger fraction of the light exiting the tissue at angles exceeding the collection angle of the fiber, given by its numerical aperture, which in turn translates into a lower signal amplitude.

Table 1 classifies the results as a function of vessel BP, with successful seals meeting or exceeding the industry test standard of 360 mmHg. Differences in BP and percentage decrease in optical power transmission were both statistically significant ($p < 0.01$). There was no statistical difference in blood vessel diameters between test groups ($p > 0.01$), as designed.

Optical diffuse transmission using IR laser ($\lambda = 1470$ nm)

Figure 6 shows the erratic signal acquired when the high-power therapeutic beam at 1470 nm is used for diagnostic feedback as well. The data were inconsistent and unreliable due in part to competing changes in the dynamic tissue optical properties. For example, the water absorption coefficient decreased upon tissue dehydration during laser heating, translating into an increase in the optical transmission signal. However, the scattering coefficient increased upon tissue coagulation, translating into a decrease in the optical transmission signal as well.

DISCUSSION

Results of the real-time diffuse optical transmission measurements demonstrated the ability to non-destructively predict successful vessel seals (≥360 mmHg). The increase in the scattering coefficient for a successfully sealed blood vessel corresponded to an approximately 59% loss in transmitted power. This percent difference is higher than the MC model predicted. The discrepancy originates in part from the model using absorption and scattering coefficients derived from existing literature, for human aorta thermally damaged at a temperature of 100°C, while the vessel must experience a much higher temperature range of 200–300°C to achieve a successful seal.[21] This temperature difference accounts for the higher scattering and greater decrease in signal during the experiments. It may also account for the percent change in transmitted power for seal failures closely correlating with the calculated value, since the maximum temperature reached in these failed samples is closer to the 100°C used in the scattering coefficient estimation for the MC simulations. It should also be noted that the difference between the room temperature tissue studies (20°C) and normal body temperature (37°C) is insignificant given that a range of temperatures between 200 and 300°C is necessary for a successful seal.

Another factor in the discrepancy between the MC model simulation results and the experimental results involves the numerical aperture of the collection fiber. The simulations do not incorporate an aperture to filter out light at scattered angles that are too large for the fiber to collect. This factor also contributes in part to the larger decrease in signal measured during the experiments.

The 635-nm visible aiming beam is preferable to the 1470-nm IR beam for real-time diagnostic feedback, for several reasons. First, the 635-nm beam was operated at low power, thus enabling a safe and simple means to acquire a calibrated, baseline starting signal for each individual blood vessel of variable diameter. This is an important criterion, since the marker for a successful seal is observed by a relative measurement in the form of a percent change. Since the 1470-nm laser is operated at

Evaluation criteria	Vessel size (mm)	Mean BP (mmHg)	ΔPower (%)	Sample size (n)
Success (BP ≥ 360)	3.3 ± 1.0	592 ± 248	59 ± 11	12
Failure (BP < 360)	2.4 ± 0.7	19 ± 12	23 ± 8	12
Significance	$p = 0.03$	$p = 2.6E{-}5$	$p = 5.4E{-}8$	

Abbreviation: BP, burst pressure.

TABLE 1 Decrease in optical power transmission at the visible wavelength of $\lambda = 635$ nm for successful seals (BP ≥ 360 mmHg) and failed seals (BP < 360 mmHg).

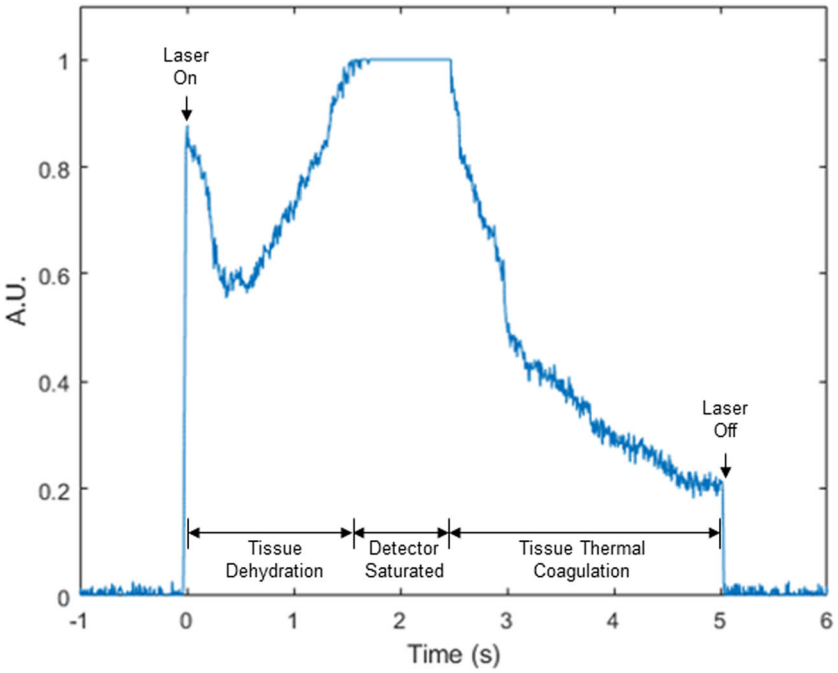

FIGURE 6 Representative real-time optical power transmission data during the sealing procedure, using high-power therapeutic 1470-nm wavelength as the diagnostic beam. At $t = 0$ seconds, the laser is activated, leading to an instantaneous rise in the signal. The erratic signal between $t = 0$ and 5 seconds can be attributed in part to different contributions and time scales of competing changes in the dynamic tissue optical properties: increased transmission due to tissue dehydration (lower absorption coefficient) and decreased transmission due to tissue coagulation (increased scattering coefficient). Loss of signal in the range of $t = 1.5$–2.5 seconds is due to saturation at the detector setting. A.U., arbitrary unit.

high power, it is impossible to safely collect a baseline transmission signal before beginning the procedure. Any high-power laser beam should be filtered out, thus requiring the use of two different wavelengths for the therapeutic and diagnostic arms of this study.

Second, the 635-nm beam is preferable for diagnostic purposes because its wavelength avoids a major water absorption peak in soft tissues. The major water absorption peak present at 1450 nm prevents reliable real-time diagnostics using the 1470-nm diode laser. At 1470 nm, a large initial spike in the data was observed after the tissue became dehydrated during laser irradiation, which resulted in an inherently unstable transmission signal, in turn making analysis inconsistent and unpredictable (Figure 6). The problem is that tissue hydration level is altered within a tissue sample during rapid laser heating and associated dehydration, and total water content may also vary considerably among tissue samples as well due to different vessel thicknesses or diameters.

Third, the diagnostic setup using the 635-nm beam enabled the high-power, 1470-nm beam to be completely filtered out before detection, using a short-pass filter. Any potential risk of laser-induced damage to the detector from direct incidence of the high power 1470 nm beam was therefore eliminated.

There are several limitations to this study. First, all experiments were performed utilizing a bulk optics setup, which is not practical for clinical use. This technology will need to be miniaturized for integration into a standard laparoscopic device and Maryland jaw configuration, as the next step in its development, before in vivo tests can be performed. To aid in this process, a smaller collection fiber may be necessary, which could potentially make the signal collection more difficult, unless an even larger NA can be used to compensate for the smaller fiber core diameter.

A second limitation concerns the fixed laser beam length used for all blood vessels, regardless of their diameter. In practice, the use of a fixed laser beam length may result in partial overflow of the beam when incident on smaller diameter blood vessels, in turn corresponding to an initially inflated optical power transmission signal. In future laparoscopic devices, an approach using adjustable beam lengths may be utilized for different vessel diameters, to compensate for this limitation, as recently demonstrated using a reciprocating side-firing fiber design with a programmable and adjustable scan length.[23]

CONCLUSIONS

This preliminary study demonstrated that a non-destructive method utilizing the collection of diffuse optical transmission of scattered visible (635 nm) light through a blood vessel consistently predicted a strong vessel seal during irradiation and thermal coagulation

with a high-power IR laser (1470 nm). With further development, the fiber optic collection component of the real-time diffuse optical transmission feedback system may be integrated into the laparoscopic device jaw. The detector and larger optical components may be integrated into the device handle, potentially providing a simple, inexpensive, and automated method of deactivating the laser once successful seals are achieved. These studies provide the foundation for the development of a laparoscopic device that has the capability both to seal blood vessels and provide real-time feedback using only optical-based methods.

ACKNOWLEDGMENTS

This study was supported by the National Institute of Biomedical Imaging and Bioengineering of the National Institutes of Health, under Grant R15EB028576. Nicholas C. Giglio was supported by a Lucille P. and Edward C. Giles Dissertation-Year Graduate Fellowship. The authors thank Dr. Thomas C. Hutchens for his assistance.

CONFLICTS OF INTEREST

The authors declare no conflicts of interest.

ORCID

Nathaniel M. Fried https://orcid.org/0000-0003-1275-7716

REFERENCES

1. Blencowe NS, Waldon R, Vipond MN. Management of patients after laparoscopic procedures. BMJ. 2018;360:k120.
2. Kennedy JS, Stranahan PL, Taylor KD, Chandler JG. High-burst-strength, feedback-controlled bipolar vessel sealing. Surg Endosc. 1998;12(6):876–8.
3. Shigemura N, Akashi A, Nakagiri T, Ohta M, Matsuda H. A new tissue-sealing technique using LigaSure system for nonanatomical pulmonary resection: preliminary results of sutureless and stapleless thoracoscopic surgery. Ann Thorac Surg. 2004;77(4):1415–8.
4. Patrone R, Gambardella C, Romano RM, Gugliemo C, Offi C, Andretta C, et al. The impact of the ultrasonic, bipolar and integrated energy devices in the adrenal gland surgery: literature review and our experience. BMC Surg. 2019;18(Suppl 1):123.
5. Cilip CM, Rosenbury SB, Giglio NC, Hutchens TC, Schweinsberger GR, Kerr D, et al. Infrared laser fusion of blood vessels: preliminary ex vivo tissue studies. J Biomed Opt. 2013;18(5):058001.
6. Giglio NC, Hutchens TC, Perkins WC, Latimer CA, Ward A, Nau WH, et al. Rapid sealing and cutting of porcine blood vessels, ex vivo, using a high power, 1470-nm laser. J Biomed Opt. 2014;19(3):038002.
7. Hardy LA, Hutchens TC, Larson ER, Gonzalez DA, Chang CH, Nau WH, et al. Rapid sealing of porcine renal vessels, ex vivo, using a high power, 1470-nm laser, and laparoscopic prototype. J Biomed Opt. 2017;22(5):058002.
8. Cilip CM, Kerr D, Latimer CA, Rosenbury SB, Giglio NC, Hutchens TC, et al. Infrared laser sealing of porcine vascular tissues using 1470 nm diode laser: preliminary in vivo studies. Lasers Surg Med. 2017;49(4):366–71.
9. Floume T, Syms RA, Darzi AW, Hanna GB. Real-time optical monitoring of radio-frequency tissue fusion by continuous wave transmission spectroscopy. J Biomed Opt. 2008;13(6):064006.
10. Floume T, Syms RA, Darzi AW, Hanna GB. Optical, thermal, and electrical monitoring of radiofrequency tissue modification. J Biomed Opt. 2010;15(1):018003.
11. Su L, Fonseca MB, Arya S, Kudo H, Goldin R, Hanna GB, et al. Laser-induced tissue fluorescence in radiofrequency tissue-fusion characterization. J Biomed Opt. 2014;19(1):015007.
12. Su L, Cloyd KL, Arya S, Hedegaard MAB, Steele JAM, Elson DS, et al. Raman spectroscopic evidence of tissue restructuring in heat-induced tissue fusion. J Biophotonics. 2014;7(9):713–23.
13. Giglio NC, Fried NM. Optical transmission feedback for infrared laser sealing of blood vessels. Proceedings of the OSA/SPIE European Conferences on Biomedical Optics; 2021.
14. Jasiński M. Numerical analysis of soft tissue damage process caused by laser action. AIP Conf Proc. 2018;1922:060002.
15. Nagarajan VK, Gogineni VR, White SB, Yu B. Real time evaluation of tissue optical properties during thermal ablation of ex vivo liver tissues. Int J Hyperthermia. 2019;35(1):176–82.
16. Ritz JP, Roggan A, Isbert C, Muller G, Buhr HJ, Germer CT. Optical properties of native and coagulated porcine liver tissue between 400 and 2400 nm. Lasers Surg Med. 2001;29(3):205–12.
17. Chan EK, Sorg B, Protsenko D, O'Neil M, Motamedi M, Welch AJ. Effects of compression on soft tissue optical properties. IEEE J Sel Top Quantum Electron. 1996;2(4):943–50.
18. Cilesiz IF, Welch AJ. Light dosimetry: effects of dehydration and thermal damage on the optical properties of the human aorta. Appl Opt. 1993;32(4):477–87.
19. Marti D, Aasbjerg RN, Andersen PE, Hansen AK. MCmatlabL an open-source, user-friendly, MATLAB-integrated three-dimensional Monte Carlo light transport solver with heat diffusion and tissue damage. J Biomed Opt. 2018;23(12):1–6.
20. Jacques SL. Monte Carlo modeling of light transport in tissues (steady state and time of flight). In: Welch AJ, van Gemert MJC, editors. Optical–thermal response of laser-irradiated tissue. Heidelberg: Springer; 2011. p. 109–44.
21. Giglio NC, Fried NM. Computational simulations for infrared laser sealing and cutting of blood vessels. IEEE J Sel Top Quantum Electron. 2021;27(4):1–8.
22. Prahl SA, Keijzer M, Jacques SL, Welch AJ. A Monte Carlo model of light propagation in tissue. Proc SPIE. 1989;10305:102–11.
23. Giglio NC, Grose HM, Fried NM. Comparison of fiber-optic linear beam shaping designs for laparoscopic laser sealing of vascular tissues. Opt Eng. 2022;61(2):026112.

How to cite this article: Giglio NC, Fried NM. Nondestructive optical feedback systems for use during infrared laser sealing of blood vessels. Lasers Surg Med. 2022;54:875–882. https://doi.org/10.1002/lsm.23548